Adsorbate-adsorbate interactions from statistical analysis of STM images: N/Ru(0001)

J. Trost, T. Zambelli, J. Wintterlin, and G. Ertl

Fritz-Haber-Institut der Max-Planck-Gesellschaft, Faradayweg 4-6, 14195 Berlin, Germany

Atomic nitrogen on Ru(0001) was prepared by dissociative chemisorption of N_2 and studied by scanning tunneling microscopy (STM) at 300 K. Nitrogen occupies the hcp threefold hollow site and is imaged as a depression with a diameter of about 5 Å. Interactions between the adsorbed nitrogen atoms were obtained by statistical analysis of STM images, by extraction of the two-dimensional pair distribution function from the arrangement of the N atoms. Since the nearest-neighbor separations could be identified with atomic precision, the pair distribution function g and hence the potential of mean force V_{eff} were obtained as a function of the discrete neighbor sites j up to the tenth nearest neighbor. A comparison with Monte Carlo calculations for balls with a hard-sphere potential provides information about the pair potential $V_{pair}(j)$: The nearest-neighbor site is strongly repulsive, the second-neighbor site is weakly repulsive, and the third-neighbor site is weakly attractive. These findings rationalize the absence of island formation and of a well-ordered 2×2 phase for the N/Ru(0001) system: At temperatures ≥ 300 K the attractive interaction on the third-neighbor site is too weak, while at lower temperatures the diffusion barrier of 0.9 eV represents a kinetic obstacle. The fact that the range of the interaction is identical to the diameter of the N-atom features in the STM topographs is taken as evidence that the interaction is caused by substrate-mediated electronic forces. [S0163-1829(96)04348-2]

I. INTRODUCTION

Interactions between adsorbed particles on solid surfaces play a central role in surface science. Together with the adsorbate-substrate potential they determine the formation of surface phases, e.g., of ordered structures of atoms or molecules, the mobility of adparticles, and the mechanisms and activation energies of chemical reactions between adsorbed particles. Knowledge of these interactions is therefore of fundamental importance for the understanding of catalytic reactions.[1,2] Interactions between adsorbed particles can be divided into direct interactions, comprising van der Waals and orbital overlap[3] as well as electrostatic interactions[4] and indirect ones, namely, substrate-mediated electronic[5,6] and elastic interactions.[7] For a particular system the relative importance of the different contributions is mostly unknown, as is the range over which the interactions extend laterally. The main problem is that for the majority of systems no quantitative experimental data are available. In principle, values for interaction energies can be extracted from measurements of the coverage dependence of adsorption energies which may be obtained by temperature programmed desorption (TPD),[8] measurements of isotherms,[9] or microcalorimetry.[10] However, these methods do not provide the distance dependence of the interactions, and a quantitative analysis of the TPD data, which are mostly the only ones available, is not unequivocal. Scattering experiments that yield distribution functions that contain information about the particle-particle potential are used for fluids in three dimensions,[11] but, to our knowledge, have not been applied to evaluate interactions between particles on surfaces. Pair potentials between adsorbates, however, could be obtained in a very direct way by means of field ion microscopy,[12–15] by determination of the pair distribution function of two atoms adsorbed on a tip.

Unfortunately, this method is restricted to adsorbed metal atoms. An alternative approach consists of an experimental determination of phase diagrams and their Monte Carlo modeling with the interaction energies as adjustable parameters. This, however, has been restricted so far to only few examples.[16]

In this paper we present an investigation based on a microscopic determination of interactions between adparticles, by means of scanning tunneling microscopy (STM). The method is based on an evaluation of the radial distribution function $g(r)$ (r is the distance between the particles) from STM images, which provides the potential of mean force $V_{eff}(r)$. A comparison with results from additional Monte Carlo calculations allows one to estimate to what extent this describes also the desired pair potential $V_{pair}(r)$. STM has been applied before in a qualitative fashion to obtain interactions between adsorbed O atoms on Ni(100) by Kopatzki and Behm,[17] who found repulsive interactions at nearest- and next-nearest-neighbor sites and an attraction at third-nearest-neighbor sites. Our present study on N atoms adsorbed on Ru(0001) allows, in addition, one to give quantitative estimates about the underlying energies.

For an exact description of a many particle system one has to consider pair and all higher-order interactions. However, at low concentrations, as they were used in the present study, taking only pair interactions into account is expected to be a good approximation and we shall discuss our results neglecting third- and all higher-order interactions. The paper completes our STM study on N/Ru(0001), for which recently we have presented results about the surface diffusion of nitrogen.[18] N atoms adsorbed on Ru(0001) form 2×2 and $(\sqrt{3}\times\sqrt{3})R30°$ structures at coverages of 0.25 and 0.33, respectively,[19] for which a recent low-energy electron diffraction (LEED) analysis revealed the occupation of three-

fold hcp sites on a nonreconstructed substrate.[20]

II. EXPERIMENT

The experiments were performed in a UHV system containing the STM described in an earlier paper[21] and commercial Auger electron spectroscopy (AES), LEED instruments, and an ion gun for sputter cleaning of the sample. The base pressure of the system is below 1×10^{-10} mbar. STM images were recorded at room temperature and tunneling parameters are given in each figure caption with the sample bias with respect to the tip potential. The Ru(0001) surface was prepared by sputtering and annealing cycles. For this purpose the annealing temperature was successively increased to ≈ 1400 K, taking care that the level of carbon contamination at the surface did not rise. After this temperature had been reached surface carbon was removed, without further sputtering, by reaction with oxygen to CO, which desorbs from the surface. This was achieved by repeated dosing with 10 L of oxygen and annealing (1 L = 1.33×10^{-6} mbar s). The surface was regarded to be clean, when, after annealing to 1750 K, no carbon could be detected with STM and AES. We mention that several thousand cleaning cycles were necessary to reach this point.

Because of the low sticking probability for dissociative adsorption of N_2 the gas inlet system has to meet special requirements. First, gases as pure as possible have to be used, which, second, have to be kept free from contaminants. This was achieved by a design that is based upon the work of Shi, Jacobi, and Ertl.[22] N_2 of the highest commercially available purity (>99.9999 vol %) was used. In order to preserve this purity only UHV compatible parts were used on the high-pressure side of the gas inlet, i.e., CF flanges and inside polished pipes and fittings of high-grade steel. For pressure reduction from the gas bottle no commercial regulator was used because of a possible contamination by the capillaries inside the manometers. Instead, a small volume of the gas (4.7 cm^3, 200 bar) was expanded into a larger volume (94 cm^3), which was connected to the UHV chamber with a leak valve. Initially, the gas inlet had been baked out and evacuated with a turbo pump. Additionally, one point of the gas inlet system was connected to a liquid-nitrogen container to freeze out remaining contaminant gases while dosing. Nitrogen was adsorbed at a crystal temperature of 500 K, where the adsorption of the main contaminant CO is suppressed. By this procedure exposures of 10^6 L of N_2 could be applied without contaminating the surface.

Although the dissociative sticking coefficient for N_2 at 300 K is only of the order of 10^{-12},[23] considerable coverages could be reached with exposures of only about 10^4 L when some filament in the UHV chamber was left on.[24] This has to be attributed either to dissociation or to some excitation of the N_2 molecules at the filament. Dissociation appears less likely since the mean free path at the typical dosing pressure of 5×10^{-5} Torr is between 1 and 2 m. An N atom collides therefore with a high probability with the chamber walls before reaching the sample and gets trapped. Since no pressure dependence of the sticking probability was found, also collisions of the atoms with N_2 molecules are ruled out since the mean free path is inversely proportional to pressure. We prefer therefore an explanation whereafter an excited N_2^* spe-

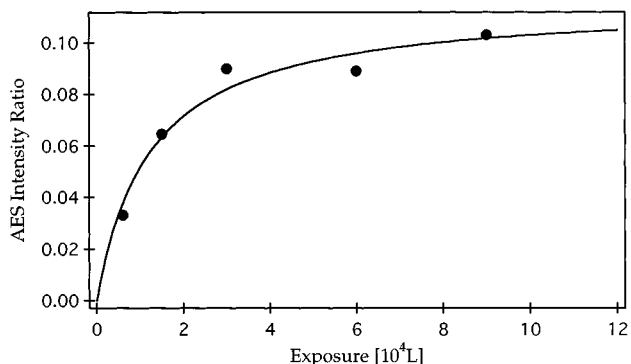FIG. 1. Nitrogen uptake curve with the ion gauge filament left on. Ratio of AES peak to peak intensities of nitrogen and ruthenium N(384 eV)/Ru(231 eV) vs N_2 exposure. The curve is a fit to the data (dots), assuming second-order adsorption. Experimental parameters are crystal temperature, 500 K; N_2 pressure, 5×10^{-5} Torr; primary AES electron energy, 3.0 keV.

cies is produced at the hot filament, which survives several collisions with the chamber walls and finally dissociates on the Ru(0001) surface. The sticking probability was of the order of 10^{-5} (with respect to the combined $N_2^* + N_2$ exposure) under the applied conditions. At this point we can only speculate about the nature of the N_2^* species. It might be an electronically excited molecule since such a species was reported to have lifetimes of the order 10^{-1} s as a component in *active nitrogen*.[25] For practical reasons, the filament of the ionization gauge was used since it turned out that this could be degassed best. With this procedure nitrogen layers nearly free of contaminants could be produced: After an exposure of 9×10^4 L of N_2 at 500 K only nitrogen was detected in the Auger spectra (e.g., for oxygen the detection limit is $\Theta_O \approx 0.01$). The nitrogen uptake curve at 500 K is displayed in Fig. 1. It is seen that saturation is nearly reached. The corresponding absolute coverage is $\Theta \approx 0.25$ as we conclude from STM data not shown here. In this case a poorly ordered overlayer containing small 2×2 patches is observed. Higher coverages (up to $\Theta = 0.47$) can be reached by exposure and decomposition of NH_3.[19]

III. RESULTS

A. The N/Ru(0001) adsorbate complex

An STM topograph of the Ru(0001) surface (recorded at 300 K) after exposure to 6×10^3 L of N_2 at 500 K is shown in Fig. 2. Black dots represent individual N atoms, i.e., nitrogen is imaged as a depression, which is largely independent of the bias voltage. The imaging depth is 0.3–0.4 Å for tunneling resistances between 2×10^7 and 6×10^8 Ω. The mean diameter of the atomic features is about 5 Å. Since this value is much greater than the nitrogen Pauling diameter of 1.4 Å it is clear that the STM does not "see" the N atom alone but the adsorbate complex, consisting of the N atom and neighboring Ru atoms. The imaging properties of nitrogen are similar to oxygen, which is also imaged as depressions. This is consistent with predictions by Lang,[26] which are based on calculated changes of the density of states of a jellium surface caused by an adsorbed oxygen atom. It is found that electronic charge is shifted from the metal to the
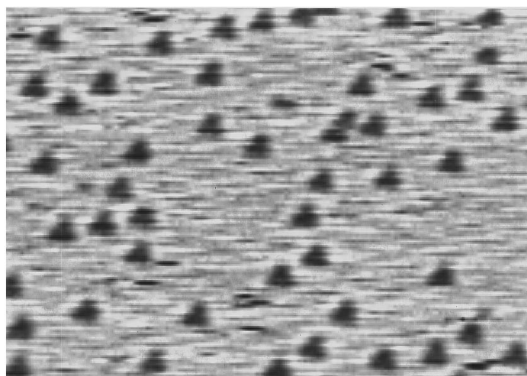
FIG. 2. STM topograph of the Ru(0001) surface after exposure of 6×10^3 L of N_2 at 500 K. Tunneling parameters are 86×54 Å^2, -0.6 V, and 30 nA.
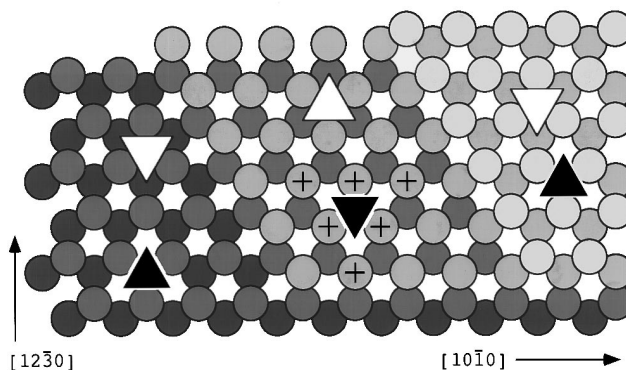

FIG. 4. Model of the Ru(0001) surface, showing four layers with two atomic steps. The orientation of fcc (white) and hcp (black) sites changes on successive terraces. For one hcp site the Ru atoms that form the adsorbate complex with the N atom are marked by crosses.

O atom, which is located in O $2p$ states about 7 eV below E_F and thus does not contribute to the tunnel current. On the other hand, at E_F, the charge redistribution causes a decrease of the density of states and thus a reduced tunnel current. For atomic nitrogen on iron, nickel, and copper surfaces electron spectroscopy showed that the N $2p$ band is located 5–6 eV below E_F,[27–29] i.e., at energies similar to those for oxygen. Since for Ru surfaces a very similar electronic structure is expected, the imaging properties are therefore in qualitative agreement with theory. We mention, however, that in recent STM studies of atomic nitrogen on Cu(100) (Ref. 30) and Ni(100),[31] both depressions and protrusions were observed, depending on tunneling parameters and on the tip state. This shows once more that STM imaging of adsorbates is not fully understood yet.

The N/Ru adsorbate complexes have a triangular shape as is seen in Figs. 2 and 3. These triangles have all the same

orientation when on the same terrace. The orientation alternates, however, on successive terraces, as seen in Fig. 3, which shows a STM image after exposure of 1.2×10^4 L of N_2 at 500 K. This observation excludes imaging artifacts caused by a special atomic configuration at the tip since both orientations are imaged equally well. We conclude that nitrogen occupies only one type of adsorption site, which must be a threefold site because of the imaging symmetry. The alternation of the orientation is explained by the model shown in Fig. 4: Because of the hcp structure of Ru both fcc and hcp sites change their orientation on successive terraces. To decide which site, fcc or hcp, is occupied images of coadsorbed nitrogen and oxygen atoms (formed by dissociation of NO molecules) were recorded. The adsorption site of oxygen is known to be the hcp site from a LEED $I(E)$ study.[32]
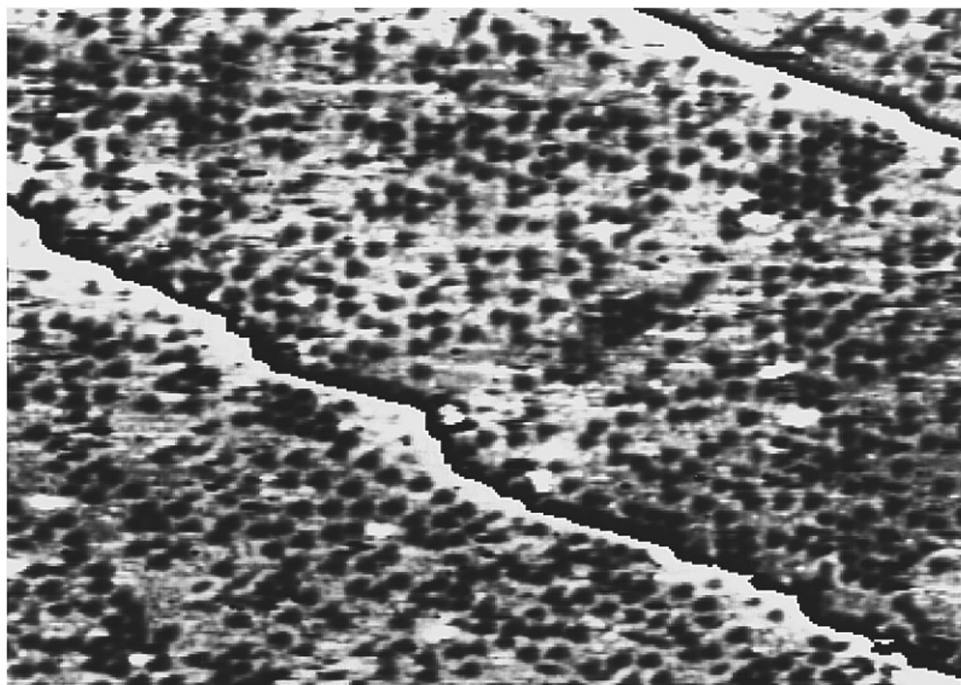

FIG. 3. STM topograph of the Ru(0001) surface after exposure of 1.2×10^4 L of N_2 at 500 K. Diagonal lines are two monoatomic steps. Tunneling parameters are 228×190 Å^2, -0.6 V, and 10 nA.
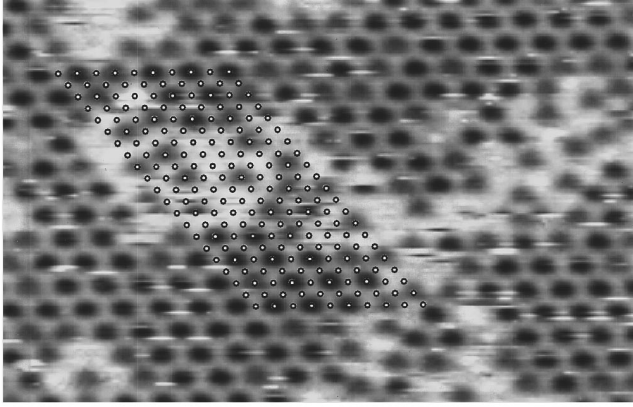
FIG. 5. STM topograph of the Ru(0001) surface after exposure of 1.5 L of NO at room temperature. O atoms are imaged deeper (black) than N atoms (gray). Small dots indicate the lattice of hcp sites, using the O atoms in the 2×2 areas as fix points. Tunneling parameters are 89×80 Å^2, -0.3 V, and 33 nA.

Figure 5 shows the surface after exposure to 1.5 L of NO. Two different species can be identified by the imaging depth: The deeper features (black) are O atoms, the others (gray) are N atoms. This discrimination is based on the observation that the mobility of oxygen at low coverages, where mainly single atoms are present, is more than two orders of magnitude larger than that of nitrogen.[18] It turns out that the more mobile species is imaged deeper than the less mobile one. Additionally, oxygen is known to form 2×2 islands,[33] in contrast to nitrogen. This 2×2 structure is seen in Fig. 5 as an ordered, hexagonal pattern, however, with some nitrogen atoms incorporated. Between the 2×2 covered areas additional, individual nitrogen atoms are located. Since the positions of the dark, i.e., oxygen, atoms in the 2×2 areas define the lattice of hcp sites, the positions of the N atoms are obtained by extrapolating the lattice to the area between the 2×2 patches. This is demonstrated in Fig. 5 by the point lattice. It turns out that all of the N atoms, those within the islands and the single ones, occupy the same sites as the O atoms. The N adsorption site is thus identified as the hcp site. This conclusion is in agreement with the results of a recent LEED analysis and density-functional calculations.[20] This justifies the lattice-gas model underlying the following analysis.

B. Interactions between adatoms

The interaction potential between the adsorbed nitrogen atoms was evaluated as a function of distance by statistical analysis of images such as Fig. 3. In the absence of a substrate lattice the interaction potential is a continuous function of distance between the particles, as it is realized, e.g., by intermolecular forces in three-dimensional gas phases.[34] For *continuous* two-dimensional systems the radial distribution function as a function of the distance r is defined as

$$g(r)=(N\rho)^{-1}\sum_{i=1}^{N}\frac{n_i(r,dr)}{2\pi r dr}, \qquad (1)$$

where $n_i(r,dr)$ is the number of particles in a shell of radius r and thickness dr around the ith particle, ρ is the particle
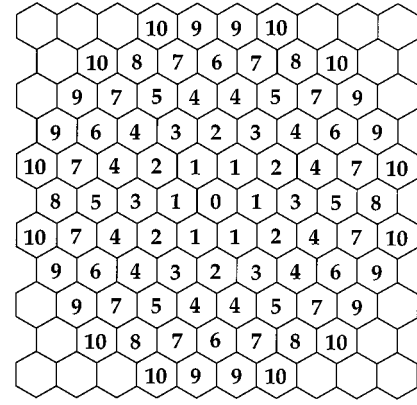

FIG. 6. Hexagonal lattice of cells, each cell corresponding to a hcp site. Numbers mark the index j of the distance between an atom in the center and an atom in the respective cell.

density, and N the total number of particles. In the present case of a lattice-gas system with defined adsorbate sites the interaction potential between adsorbed particles is discrete. For the hexagonal lattice of hcp sites on Ru(0001) the distances are $r_0=0$, $r_1=1$, $r_2=\sqrt{3}$, $r_3=2$, $r_4=\sqrt{7}$, $r_5=3$, $r_6=2\sqrt{3}$, $r_7=\sqrt{13}$, $r_8=4$, $r_9=\sqrt{19}$, $r_{10}=\sqrt{21}$, ..., all in units of the lattice constant. This is illustrated in Fig. 6, where each cell represents a hcp site around an atom located in the center. For such a two-dimensional *lattice-gas* system the pair distribution function at the jth-nearest-neighbor site can be defined as

$$g(j)=(N\Theta)^{-1}\sum_{i=1}^{N}\frac{n_i(j)}{m(j)}, \qquad (2)$$

where $n_i(j)$ is the number of jth-nearest-neighbor particles around the ith particle, Θ the coverage, and $m(j)$ the number of jth-neighbor sites. The normalization, by division of ρ and Θ, respectively, makes $g(r)$ and $g(j)$ unity when r and j approach infinity. The meaning of the pair distribution function is that deviations from a random particle distribution manifest themselves in deviations from $g=1$. From the definition Eq. (2) the pair distribution function at a certain site j can be interpreted as the ratio of two probabilities, the probability to find a particle at that site divided by the average occupation probability. At equilibrium a ratio of occupation probabilities should be Boltzmann distributed, viz.,

$$g(j)=e^{-V_{\text{eff}}(j)/kT}. \qquad (3)$$

The effective interaction potential $V_{\text{eff}}(j)$ is the so-called *potential of mean force*, which describes the interaction within an ensemble of particles. It is generally different from the pair potential $V_{\text{pair}}(j)$, which acts between two isolated particles. Crucial for the validity of Eq. (3) is that the system is in thermodynamic equilibrium. This prerequisite is fulfilled for the present system as follows from the diffusion parameters, which had been determined before.[18] For low coverages, of the order of $\Theta\approx0.1$, as it is the case in Figs. 2 and 3, equilibrium should be reached when each N atom has moved over a distance of more than ten times the mean neighbor separation, i.e., about 100 Å. With a diffusion coefficient of $D=4\times10^{-18}$cm^2/s at 300 K the time for a dif-
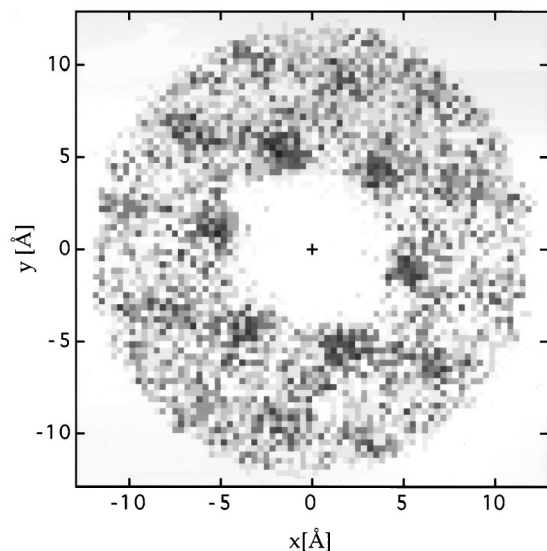
FIG. 7. Two-dimensional pair distribution function at a nitrogen coverage of $\Theta = 0.095$. Each point corresponds to a certain pair of N atoms. Six spots with enhanced point density are visible at a distance of about 5.5 Å, which reflect an increased probability to form third-neighbor distances.

fusion length of 100 Å would be about one day. However, since the adsorption was carried out at 500 K this time reduces to a fraction of a second as can be estimated from the diffusion barrier. Here it is assumed that no islanding occurs that would require long-range mass transport before equilibrium is established. It will turn out that this is the case.

In order to extract the pair distribution function from STM images one has to be able to determine precisely the sites j at which the occupation probability is then evaluated. Since the STM data of N/Ru(0001) usually do not show the atomically resolved substrate, direct identification of j values is not possible. However, the distances could still be determined with atomic resolution as shown by the two-dimensional pair distribution function in Fig. 7 for which a larger image containing 1344 N atoms was analyzed. For this the distance vector of each pair of atoms was evaluated. Since, because of the pixel resolution of that image of 0.33 Å, many vectors would fall on each other, a Gaussian noise with a rms value of 0.33 Å was applied to them. All further analysis was, however, done with the original data, without noise. The vector density was then visualized by gray levels where dark areas reflect high densities (the distance between two pixels is 0.33 Å). Obviously, small distances up to about 3 Å do not occur. This corresponds to a repulsive part of the nearest-neighbor interaction. Enhanced point density can be seen at the corners of a hexagon at a distance of about 5.5 Å. This corresponds to an increased probability to form third-nearest-neighbor distances to which, e.g., the small 2×2 clusters visible in Fig. 3 contribute. Hence, although the Ru substrate lattice is not resolved in the STM image, the distance and the orientation of the six third-nearest-neighbor sites are clearly resolved in the two-dimensional (2D) pair distribution function. This allows one to map out the substrate lattice in the 2D pair distribution function and to identify all other neighbor sites. Practically, the honeycomb lattice shown in Fig. 6, where each cell represents a hcp site,
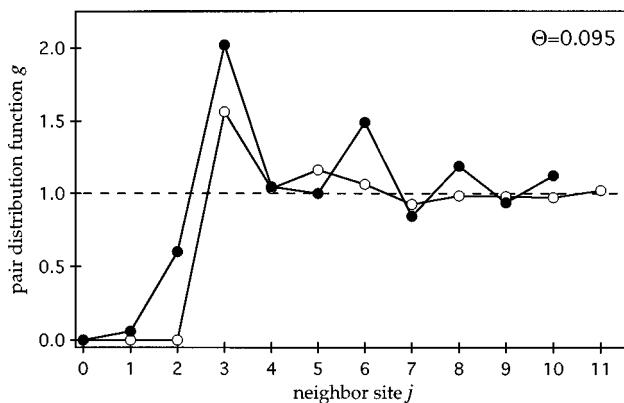

FIG. 8. Pair distribution function g vs neighbor site j obtained from Fig. 7 (black dots) and Monte Carlo calculation for hard spheres that block the first- and second-neighbor site (white dots).

was laid over the 2D pair distribution function of Fig. 7 and the number of points counted in each hexagon. After normalization according to Eq. (2) this yields the pair distribution function $g(j)$. The result for 1344 atoms, corresponding to a coverage of $\Theta = 0.095$, is reproduced in Fig. 8 as black dots. The deviations from $g(j) = 1$ corresponding to a random distribution will be discussed below.

An experimental error arises from the scattering of the points around the exact distances leading to a spillover of some points between neighboring hexagons. The extent can be estimated from the fact that a first-neighbor distance was never observed in the STM images, but, nevertheless, $g(1) = 0.06$ is found, which has to be caused by a spillover from the $g(2)$ and $g(3)$ hexagons. Hence about 10% of the points spill over to neighboring hexagons. Another measure of the error is the spot width of the third-nearest-neighbor accumulation seen in Fig. 7, which indicates an uncertainty of ± 0.8 Å for the distance. This radius is completely within one hexagon of Fig. 6. Thus the assignment of the distances to the sites is quite good, although the substrate lattice was not resolved.

Figure 9 shows the potential of mean force that was evaluated using Eq. (3). Because of the complete absence of $j = 1$ separations (the nonzero value in Fig. 8 is caused by the experimental error) no value for $V_{\text{eff}}(1)$ can be given in Fig. 9. From an STM image that contains 1344 N atoms but not a
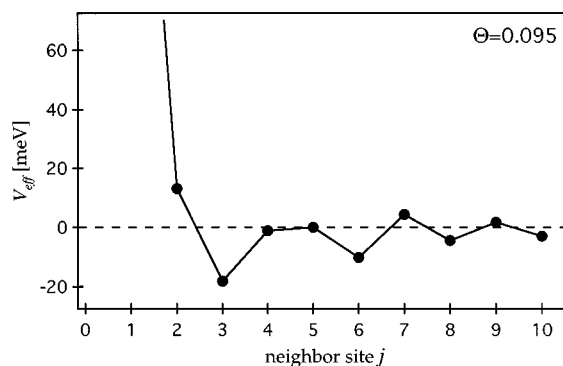

FIG. 9. Potential of mean force V_{eff} obtained from Fig. 8. Note the repulsion up to the second-neighbor site and the attractions at the third- and sixth-neighbor sites.

single nearest-neighbor distance, it is estimated that $g(1)<2.5\times10^{-4}$ and hence $V_{eff}(1)>0.2$ eV. At the second-neighbor site the potential is still repulsive, with $V_{eff}(2)=+13$ meV. Attractions are observed at the third- and sixth-neighbor sites, with $V_{eff}(3)=-18$ meV and $V_{eff}(6)=-10$ meV, respectively. This corresponds to the formation of local 2×2 order, as visible in Fig. 3. The fourth- and fifth-neighbor sites are occupied with nearly statistical probability.

IV. DISCUSSION

The above analysis yields $V_{eff}(j)$, which is not identical to $V_{pair}(j)$, the interaction potential between two individual adsorbed atoms. The connection between V_{eff} and V_{pair}, formally can be written as[35]

$$e^{-V_{eff}(j)/kT}=f(j,V_{pair},\Theta,T)e^{-V_{pair}(j)/kT}, \qquad (4)$$

with an unknown function $f(j,V_{pair},\Theta,T)$. If V_{pair} were known, f could, in principle, be calculated with the aid of statistical mechanics.[35] In general, $f=1$ when Θ approaches zero. For the present case, however, this approximation is not valid, which follows from the observation that $|V_{eff}(3)|$ still decreased when Θ was reduced. Equation (4) is equivalent to

$$V_{eff}(j)=V_{pair}(j)-Tk\ln(f), \qquad (5)$$

which leads to the interpretation of the term $k\ln(f)$ as an entropy. Thus the deviations of V_{eff} from V_{pair} are called *entropic forces*. In order to investigate to what extent entropic forces play a role at the coverages studied, Monte Carlo simulations were performed in which 4096 particles were put successively on a hexagonal lattice until a coverage of $\Theta=0.095$ was reached, the same value as in Fig. 7. For V_{pair} a hard-sphere potential was assumed, in which first- and second-nearest neighbors are blocked and the interaction at larger separations is zero. Each particle was allowed to adsorb on a randomly chosen site only when this site was not blocked by another particle.[36] In the case of blocking a new random site was chosen. The result for the pair distribution function is shown in Fig. 8 as white dots. It is clear that $g=0$ for $j=0,1,2$ because of blocking. The nearest non-blocked site is occupied with an enhanced probability $g(3)=1.56$. This is a purely entropic effect and is in agreement with the statistical-mechanics calculations.[35] The pair distribution function of the hard spheres is very similar to the experimentally determined one for the N atoms. This demonstrates, on the one hand, that at room temperature the experimental pair distribution function is quite well reproduced by a hard-sphere potential and, on the other hand, that deviations from $g=1$ to larger values at a certain distance do not necessarily originate from attractive pair interactions but may also be caused by repulsive pair interactions at other distances. It is a general difficulty to distinguish between pair interactions and entropic forces. However, since there are also differences between the experimental and the simulated data in Fig. 8 it is clear that the experimental pair distribution function cannot completely be caused by a hard-sphere potential and the corresponding entropic forces.

As already mentioned, the most striking features of the potential of mean force $V_{eff}(j)$ are repulsions at the first- and second-neighbor sites and an attraction on the third-neighbor site. This allows the following conclusions about the corresponding pair energies.

(i) Since no nearest neighbor is observed at room temperature, we conclude that the pair interaction at the nearest-neighbor distance $V_{pair}(1)$ is strongly repulsive, at least $V_{pair}(1)\gg kT=26$ meV. Entropic effects at that site caused by the interaction at the second- and third-neighbor sites are expected to be small because the energies at these sites are significantly smaller than at $j=1$. We conclude that the above estimate for the effective interaction energy at the nearest-neighbor site is valid also for the pair energy, i.e., $V_{pair}(1)>0.2$ eV.

(ii) The question to what extent the potential of mean force at the second-neighbor site, of $V_{eff}(2)=+13$ meV, is caused by pair interaction vs entropic forces is difficult to answer. The entropic forces at the second-neighbor site are predominantly affected by the first- and, to a smaller extent, by the third-neighbor site. The repulsion at the first-neighbor site leads to an entropic attraction at the second-neighbor site. Since this effect is small [for hard spheres that block only the first-neighbor site Monte Carlo calculations gave $g(2)=1.12$ for $\Theta=0.095$], we expect that the value of $+13$ meV reflects approximately the pair potential, i.e., it is slightly repulsive at the second-neighbor site. This is in accordance with the observation of Dietrich, Jacobi, and Ertl that by decomposition of NH_3 on Ru(0001) a nitrogen $(\sqrt{3}\times\sqrt{3})R30°$ structure can be prepared.[19]

(iii) Since $g(3)$ is significantly larger for the nitrogen atoms as compared to the hard spheres (see Fig. 8) it is concluded that the value $V_{eff}(3)=-18$ meV cannot be purely entropic but has an attractive contribution from the pair interaction, i.e., $V_{pair}(3)<0$. Of course, $V_{pair}(3)$ cannot exceed -18 meV, which is an upper limit for that value. This pair attraction leads, together with the entropic attraction due to first- and second-neighbor repulsion, to frequent 2×2 distances. $j=6$ is the next-nearest neighbor for a 2×2 lattice, as can be seen from Fig. 6. $V_{eff}(6)=-10$ meV is thus interpreted as an entropic effect caused by the third-neighbor attraction and reflects an increased probability to form a second 2×2 shell. Even a third 2×2 shell is visible from the attraction $V_{eff}(8)=-4.5$ meV, however, with less significance. The potential of mean force V_{eff} at larger distances can therefore be explained by the pair attraction at the third-neighbor distance.

These values can be compared to results from the literature: Recent density functional calculations for a hypothetical 1×1, a $(\sqrt{3}\times\sqrt{3})R30°$, and a 2×2 structure of nitrogen on a Ru(0001) slab[20] revealed binding energies per N atom of 4.52, 5.59, and 5.83 eV, respectively. Taking into account that there are three bonds per atom in a 2D hexagonal structure, the differences between these values correspond to repulsive pair energies of 0.36 eV at the first with respect to the second neighbor and of 80 meV at the second with respect to the third neighbor. Both values are comparable to the present results. Nearest-neighbor interactions can be extracted also from thermal desorption data. Tsai and Weinberg[37] report an almost constant N_2 desorption energy up to the maximum N coverage reached. N layers were pre-

pared by decomposition of NH_3, probably resulting in $\Theta \leq 0.25$ since only a 2×2 structure was seen.[38] The result is in agreement with our finding of only small interactions for $j \geq 2$. A drop of E_{des} at small coverages, by 3 kcal/mole, that is not reflected by our data is probably too small to be significant; the authors suspected N atoms at defects. Using a special technique for dissociative adsorption of NH_3, leading to nitrogen coverages as large as 0.47, Dietrich, Jacobi, and Ertl[19] observed N_2 desorption in two states, corresponding to 190 and 130 kJ/mole. The latter value, reflecting desorption from $j = 1$ sites, represents an upper limit since it results from decomposition of a NH species followed by prompt desorption of N_2 and H_2. ΔE_{des} corresponds to a difference of V_{pair} of greater than 0.1 eV between $j = 1$ and $j > 1$, which is consistent with our results. It is clear, however, that adsorbate-adsorbate interaction energies that are several orders of magnitude smaller than the corresponding adsorption energies cannot be evaluated accurately from differences between the latter.

Our data show that the potential of mean force can be explained by a pair potential where only the first-, second-, and third-nearest neighbors interact with nonzero energy, which gives an interaction length of $r_3 = 5.4$ Å . This value is equal to the diameter of the N/Ru adsorbate complex as it is imaged by STM (see Ru atoms marked by crosses in Fig. 4). If one brings two adsorbate complexes into contact they can interfere only at the first-, second-, and third-neighbor sites. We believe that this similarity of the interaction length and the adsorbate complex size is a strong indication that the interaction between the adsorbed N atoms is caused by a substrate-mediated electronic effect.[5,6] Each N atom modifies the surrounding Ru atoms electronically. Since this modification affects also the electron density at E_F this effect is seen by STM. van der Waals interactions, on the other hand, cannot play a dominant role in the N/Ru(0001) system because, from the nitrogen van der Waals diameter of 3.0 Å (Ref. 39) and the requirement that the atoms occupy hcp sites, the preferred nearest-neighbor distance should be the first or, less likely, the second neighbor, but *not* the third one as observed here.

Finally, from the attractive pair interaction at the third-neighbor site formation of a 2×2 structure is to be expected,

which is indeed observed at 300 K around $\Theta = 0.25$.[19] However, the fairly diffuse LEED spots indicate rather imperfect long-range order in agreement with the poor order at $\Theta = 0.25$ seen by STM. Furthermore, the STM data demonstrate that, at coverages smaller than 0.25, the N atoms do not form islands. This is in striking contrast to the behavior of adsorbed oxygen atoms on Ru(0001) for which measurements both by STM (Refs. 40 and 41) and by LEED (Ref. 33) indicate island formation. Oxygen forms also a 2×2 phase, which has the same structure. The absence of 2×2 N islands is attributed to the fact that the third-neighbor attraction between the N atoms is too small (< 18 meV). The ordering into a 2×2 structure at $\Theta = 0.25$ is therefore mainly a result of the operation of the first- and second-neighbor repulsion. Island formation at $\Theta < 0.25$ and better ordering at $\Theta = 0.25$ is, in principle, expected at lower temperatures, but there the rather high activation barrier for diffusion of 0.9 eV (Ref. 18) prevents reaching thermodynamic equilibrium.

V. CONCLUSION

In conclusion, it was shown that the potential of mean force of the nearest-neighbor interaction $V_{eff}(j)$ can be described by a pair potential $V_{pair}(j)$, which acts only at the first-, second-, and third-neighbor site. Estimates for the corresponding pair interaction energies were given explicitly. The fact that the spatial extent of interactions is the same as the range over which the electronic structure is modified is taken as evidence that the interaction is of the substrate-mediated electronic type. It was further shown that at around room temperature and low coverages the spatial distribution of the N atoms, which corresponds to V_{eff}, can be described approximately by a pair potential of hard spheres that block the first- and second-neighbor site. This fact was important for the interpretation of our diffusion data, where it was concluded that the diffusion constant is not significantly affected by nearest-neighbor interactions.[18]

ACKNOWLEDGMENT

[1] N. D. Lang, S. Holloway, and J. K. Nørskov, Surf. Sci. **150**, 24 (1985).

[2] J. K. Nørskov, in *Physics and Chemistry of Alkali Metal Adsorption*, edited by H. P. Bonzel, A. M. Bradshaw, and G. Ertl (Elsevier Science, Amsterdam, 1989), p. 253.

[3] A. Zangwill, *Physics at Surfaces* (Cambridge University Press, Cambridge, 1988).

[4] W. Kohn and K.-H. Lau, Solid State Commun. **18**, 553 (1976).

[5] T. B. Grimley, Proc. Phys. Soc. London **90**, 751 (1967).

[6] T. L. Einstein, CRC Crit. Rev. Solid State Mater. Sci. **7**, 261 (1978).

[7] K. H. Lau and W. Kohn, Surf. Sci. **65**, 607 (1977).

[8] M. Golze, M. Grunze, and W. Hirschwald, Vacuum **31**, 697 (1981).

[9] K. Christmann and J. E. Demuth, Surf. Sci. **120**, 291 (1982).

[10] N. Al-Sarraf, J. T. Stuckless, and D. A. King, Nature **360**, 243 (1992).

[11] *Simple Dense Fluids*, edited by H. L. Frisch and Z. W. Salsburg (Academic, New York, 1968).

[12] T. T. Tsong, Phys. Rev. Lett. **31**, 1207 (1973).

[13] H.-W. Fink, K. Faulian, and E. Bauer, Phys. Rev. Lett. **44**, 1008 (1980).

[14] R. Casanova and T. T. Tsong, Phys. Rev. B **22**, 5590 (1980).

[15] T. T. Tsong and R. Casanova, Phys. Rev. B **24**, 3063 (1981).

[16] L. D. Roelofs, in *Chemistry and Physics of Solid Surfaces IV*, edited by R. Vanselow and R. Howe (Springer, Berlin, 1982), p. 219.

[17] E. Kopatzki and R. J. Behm, Surf. Sci. **245**, 255 (1991).

[18] T. Zambelli, J. Trost, J. Wintterlin, and G. Ertl, Phys. Rev. Lett. **76**, 795 (1996).

[19] H. Dietrich, K. Jacobi, and G. Ertl, J. Chem. Phys. (to be published).

[20] S. Schwegmann, A. P. Seitsonen, H. Dietrich, H. Bludau, H. Over, K. Jacobi, M. Scheffler, and G. Ertl (unpublished).

[21] H. Brune, I. Wintterlin, I. Trost, G. Ertl, J. Wiechers, and R. J. Behm, J. Chem. Phys. **99**, 2128 (1993).

[22] H. Shi, K. Jacobi, and G. Ertl, J. Chem. Phys. **99**, 9248 (1993).

[23] H. Dietrich, P. Geng, K. Jacobi, and G. Ertl, J. Chem. Phys. **104**, 375 (1996).

[24] T. Matsushima, Surf. Sci. **197**, L287 (1988).

[25] Z. Bay and W. Steiner, Z. Phys. Chem. B **9**, 93 (1930).

[26] N. D. Lang, Comments Condens. Matter Phys. **14**, 253 (1989).

[27] F. Bozso, G. Ertl, M. Grunze, and M. Weiss, J. Catal. **49**, 18 (1977).

[28] H. Conrad, G. Ertl, J. Küppers, and E. E. Latta, Surf. Sci. **50**, 296 (1975).

[29] J. M. Burkstrand, G. G. Kleiman, G. G. Tibbetts, and J. C. Tracy, J. Vac. Sci. Technol. **13**, 291 (1976).

[30] F. M. Leibsle, S. S. Dhesi, S. D. Barrett, and A. W. Robinson, Surf. Sci. **317**, 309 (1994).

[31] F. M. Leibsle, Surf. Sci. **297**, 98 (1993).

[32] M. Lindroos, H. Pfnür, G. Held, and D. Menzel, Surf. Sci. **222**, 451 (1989).

[33] E. Madey, H. A. Engelhardt, and D. Menzel, Surf. Sci. **48**, 304 (1975).

[34] J. N. Israelachvili, *Intermolecular and Surface Forces* (Academic, London, 1985).

[35] T. L. Hill, *Statistical Mechanics* (McGraw-Hill, New York, 1956).

[36] It is worth noting that random number algorithms from standard libraries did not provide the expected number $g = 1$ for noninteracting particles. This requirement was fulfilled by the algorithm ran2 from Ref. 42.

[37] W. Tsai and W. H. Weinberg, J. Chem. Phys. **91**, 5302 (1987).

[38] The authors estimated a higher coverage that cannot be reconciled with the present understanding that the 2×2 structure contains only one N atom per unit cell.

[39] *CRC Handbook of Chemistry and Physics*, edited by R. C. Weast and M. J. Astle (CRC, Boca Raton, FL, 1981), Vol. 62.

[40] C. Günther, Diploma thesis, Ludwig-Maximilians-Universität München, 1989.

[41] J. Trost, S. Renisch, R. Schuster, J. Wintterlin, and G. Ertl (unpublished).

[42] W. H. Press, S. A. Teukolsky, W. T. Vetterling, and B. P. Flannery, *Numerical Recipes in C* (Cambridge University Press, Cambridge, 1992).